

**BROADBAND DIRECT DETECTION SUBMILLIMETER  
SPECTROMETER WITH MULTIPLEXED SUPERCONDUCTING  
TRANSITION EDGE THERMOMETER BOLOMETERS**

Dominic J. Benford, Troy A. Ames, Jay A. Chervenak, S. Harvey Moseley,  
Rick A. Shafer, Johannes G. Staguhn<sup>†</sup>, George M. Voellmer

*NASA Goddard Space Flight Center, Greenbelt, MD 20771, USA*

*<sup>†</sup> SSAI, Lanham, MD 20706, USA*

François Pajot, Cyrille Rioux  
*IAS-CNRS, 91405 Orsay, France*

Thomas G. Phillips  
*Caltech, Pasadena, CA 91125, USA*

Bruno Maffei  
*University of Wales, Cardiff, CF24 3YB, Wales*

Kent D. Irwin  
*NIST, Boulder, CO 80305, USA*

**Abstract**

We present performance results based on the first astronomical use of multiplexed superconducting bolometers. The Fabry-Perot Interferometer Bolometer Research Experiment (FIBRE) is a broadband submillimeter spectrometer that achieved first light in June 2001 at the Caltech Submillimeter Observatory (CSO). FIBRE's detectors are superconducting transition edge sensor (TES) bolometers read out by a SQUID multiplexer. The Fabry-Perot uses a low resolution grating to order sort the incoming light. A linear bolometer array consisting of 16 elements detects this dispersed light, capturing 5 orders simultaneously from one position on the sky. With tuning of the Fabry-Perot over one free spectral range, a spectrum covering  $\Delta\lambda/\lambda = 1/7$  at a resolution of  $\delta\lambda/\lambda \sim 1/1200$  can be acquired. This spectral resolution is sufficient to resolve Doppler-broadened line emission from external galaxies. FIBRE operates in the 350  $\mu\text{m}$  and 450  $\mu\text{m}$  bands. These bands cover line emission from the important star formation tracers neutral carbon [C I] and carbon monoxide (CO). We have verified that the multiplexed bolometers are photon noise limited even with the low power present in moderate resolution spectrometry.

## SCIENTIFIC MOTIVATION

Spectroscopy of distant galaxies in the far-infrared and submillimeter has lagged behind continuum studies at the same wavelengths (e.g., with SHARC at the CSO [1]) and spectroscopic studies at longer wavelengths (e.g. OVRO [2]). In large part, this is due to a relative lack of available instrumentation combining high sensitivity and large bandwidth. Observing an emission line from a typical galaxy with velocity-broadened linewidth of  $\sim 300\text{km/s}$  in the  $350\mu\text{m}$  and  $450\mu\text{m}$  atmospheric windows (850GHz and 650GHz, respectively) requires a spectrometer with a bandwidth of at least  $0.5\mu\text{m}$  (1GHz). Additionally, detecting this line is easiest if the spectral resolution is approximately this width. Hence, a spectrometer with a spectral resolution of slightly more than 1000 is optimal for the detection of faint galaxies in the far-infrared and submillimeter.

To put this in perspective, shown below (Fig. 1) is a 9 GHz wide portion of the high resolution spectrum of Orion-KL taken at the CSO around the CO  $J=6\rightarrow 5$  line near 690 GHz [3]. A coarse resolution spectrometer would miss the smaller features and blur the CO line, decreasing its contrast. A simulation of the spectrum of the nearby infrared-luminous galaxy M82 is shown in Fig. 2, over a 40 GHz wide portion from 790 to 830 GHz containing both the CO  $J=7\rightarrow 6$  and CI transitions. Even at a spectral resolution of 1000, the lines are resolved.

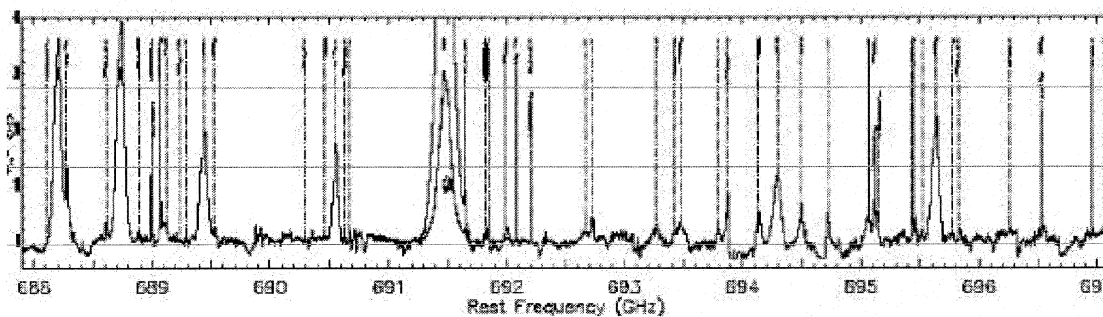


FIGURE 1. Spectrum of Orion between 688 and 697 GHz, showing many low brightness, narrow lines in addition to the dominant CO line.

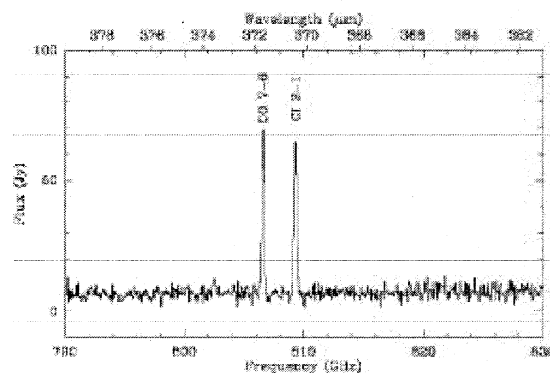


FIGURE 2. Simulated spectrum of M82 between 790 and 830 GHz, showing only the continuum and emission from CO and CI.

The Fabry-Perot Interferometer Bolometer Research Experiment, FIBRE, is an instrument designed to demonstrate a suite of advanced technologies suitable for sensitive detection of far-infrared light. This includes superconducting transition edge sensor (TES) bolometers, SQUID multiplexed amplifiers, and a cryogenic Fabry-Perot interferometer. These components are being developed for the SOFIA imaging Fabry-Perot spectrometer SAFIRE and for a complement of ground-based instruments.

Heterodyne spectrometers have been developed with noise only a few times the quantum limit at frequencies near 1THz. This is a noise temperature of order 100K. However, the photon noise from Mauna Kea in good weather using a spectral resolution of 1000 is about 46K. It is clear that in this case – indeed, whenever the instrument sees low photon occupation number – lower noise can be achieved with direct detection than with heterodyne detection [4].

## INSTRUMENT DESIGN

### Superconducting TES Bolometers and SQUID Amplifiers

The superconducting TES bolometer has been developed for use at wavelengths from the submillimeter to X-rays. It combines high speed with high sensitivity and can be read out by SQUID amplifiers, which are well suited to multiplexing. Unfortunately, the development of these detectors is too detailed to discuss at length here [5,6], but the overall technology was summarized at the 12<sup>th</sup> Terahertz Technology Symposium [7]. The FIBRE bolometers were used in the laboratory to demonstrate that multiplexed detection using the NIST-designed SQUID multiplexer of Chervenak et al. [6] was possible [8]. Further measurements, as presented by Staguhn et al. [9], have verified that the noise performance of these amplifiers is limited by detector Johnson noise contributions (e.g., amplifier noise is still below both phonon and photon noise in an appropriately designed detector) as predicted by theory.

FIBRE features two 1×8 monolithic bolometer arrays consisting of 1mm×1mm absorbers with a 50μm×150μm Mo/Cu bilayer TES. This is shown in Fig. 3.

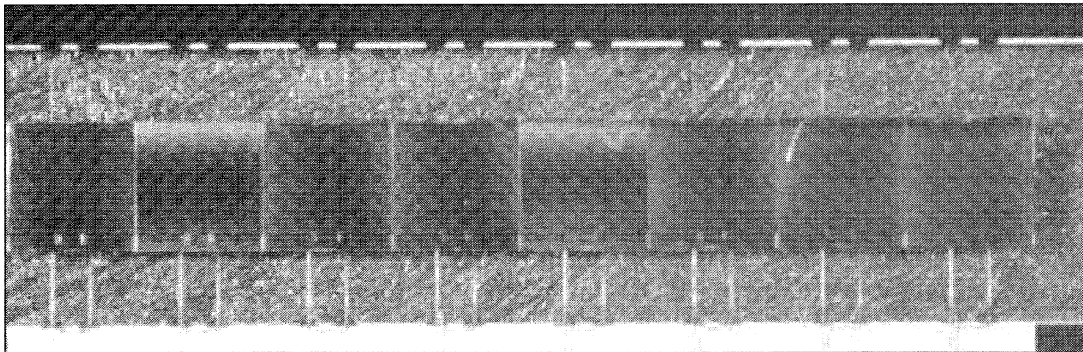


**FIGURE 3.** Photograph of a single 1×8 monolithic bolometer array. Each 1mm×1mm pixel is a 1μm thick silicon membrane supported by 4 legs approximately 5μm wide. The TES is the small pale rectangle at the bottom center of each detector.

The principal of operation of the superconducting bolometer is relatively straightforward, and similar to conventional semiconducting bolometers. A small, thermally isolated thermistor receives heat input from incident radiation and electrical bias power; the sum of these powers determines its temperature above the bath temperature (Fig. 4). The electrical bias power is simply  $P=V^2/R$ , where the resistance  $R$  depends strongly on the temperature, as shown in Fig. 5. When the incident radiation increases, the temperature rises and  $R$  increases dramatically. This causes the bias power to drop, sending the device back to the same temperature. This effect, called electrothermal feedback, is instrumental in improving the response speed, stability, linearity, and noise properties of superconducting bolometers. The noise can be made phonon-limited, where the noise equivalent power is  $NEP^2=4kT^2G$ . This noise power can be converted into a noise temperature using  $T_N = NEP/(2kv\Delta\nu)$  [10]. We have tested bolometers yielding noise temperatures of  $\sim 30\text{K}$  at frequencies of  $\sim 1\text{THz}$ , when operated from a  $^3\text{He}$  bath, and with response times of  $<2\text{ms}$ .

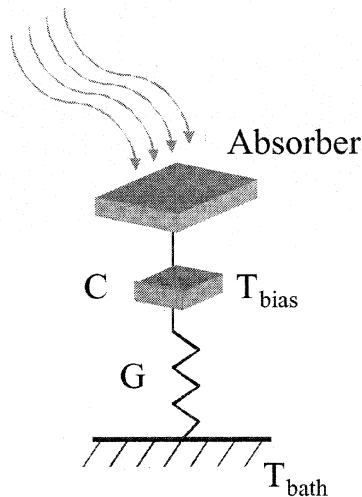


FIGURE 4. Diagram of the principal of operation of a bolometer.

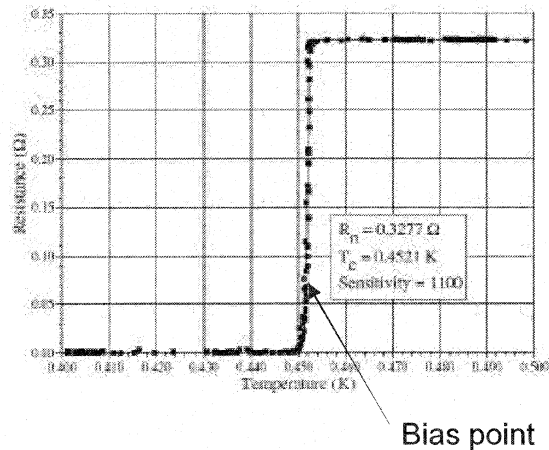


FIGURE 5. Operation of a superconducting thermistor with a sharp  $R$  vs.  $T$  curve.

### Optical Design

The optical design uses a single Fabry-Perot etalon followed by an order-sorting grating [11]. The grating is blazed to operate in its first order, which is broad enough to transmit orders 40-45 of the Fabry-Perot for  $350\mu\text{m}$  operation and orders 32-35 for  $450\mu\text{m}$  operation. The grating disperses these Fabry-Perot orders along the array such that they are separated onto adjacent sets of pixels with only slight overlap. In this manner, a spectrum consisting of several orders of the Fabry-Perot is collected simultaneously. This configuration permits spectral multiplexing by using multiple detectors, since the detectors themselves have no spectral resolving power. By stepping the Fabry-Perot over one free spectral range, a complete spectrum is accumulated. The layout of the optics and a picture of the partially assembled optical system are shown in Fig. 6. The entire assembly is shown in Fig. 7, with the detector array package and all optical/magnetic baffles in place.

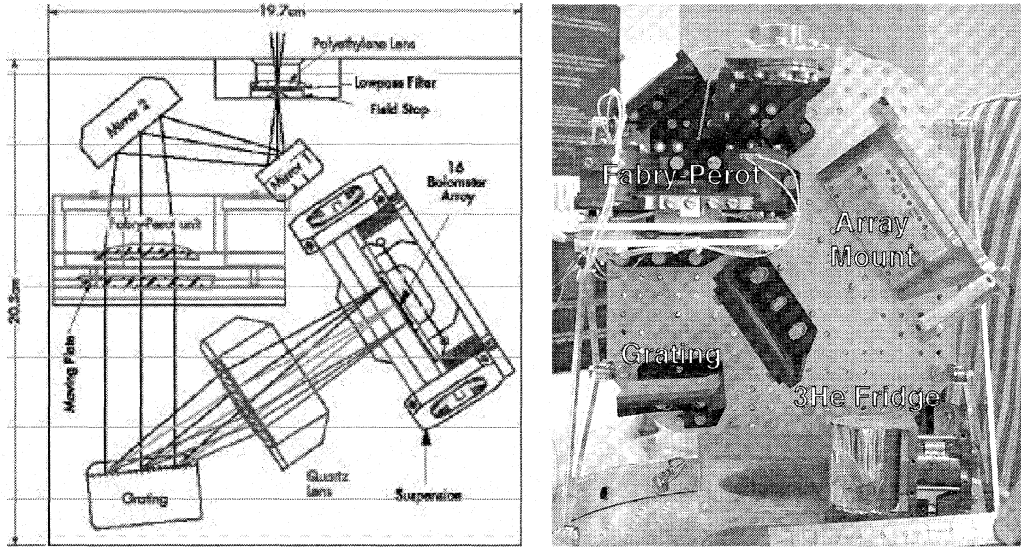


FIGURE 6. (Left) Diagram of spectrometer optics, showing three orders being dispersed onto the bolometer array. (Right) Optics being assembled, with the detector array and baffles yet to be added.

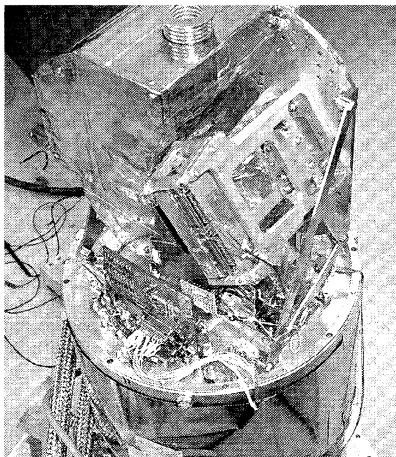


FIGURE 7. Illumination pattern of the Fabry-Perot/grating optics onto a 24-element detector array.

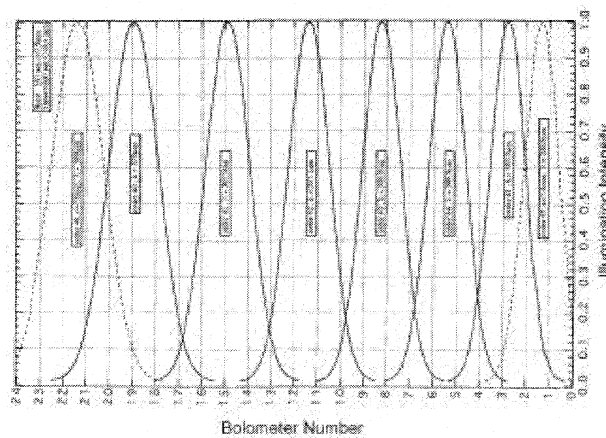


FIGURE 8. Illumination pattern of the Fabry-Perot/grating optics onto a 24-element detector array.

Instantaneously, the five to six orders are dispersed across the detector array. This illumination pattern is shown in Fig. 8. As the Fabry-Perot modulates the incident wavelengths, the peaks shift slightly, but less than two pixels width. The optics were designed to allow up to 24 pixels to be used, which cover either of the two observing bands as available from Mauna Kea. At the present, only 16 pixels are available in two groups of 8, with a gap of 3 pixels width between them. The array can be shifted in steps of 5 pixels to enable the entire band to be covered.

### Commissioning Observations

FIBRE was delivered to the Caltech Submillimeter Observatory (CSO) on Mauna Kea, Hawai'i in May-June 2001. During six nights of poor weather, the instrument was operated and found to work very well. The bolometers were read out in multiplexed fashion (Fig. 9). This scan was taken while tuning the Fabry-Perot and observing a local oscillator source. The signal is seen strongly on one channel and weakly in others, demonstrating good optical performance for spectroscopy. The position of the Fabry-Perot is also shown. Those bolometers that were illuminated at a given Fabry-Perot tuning were found to have about 20 times the noise of the dark bolometers. The expected photon noise contribution is approximately 10 times the intrinsic (phonon + Johnson) noise of the detectors, so the system noise is near the theoretical performance and the bolometers are background-limited with a net NEP of  $3 \times 10^{-17}$  W/ $\sqrt{\text{Hz}}$ .

A spectrum (Fig. 10) was taken using a local oscillator source operating at  $372 \mu\text{m}$  (807GHz). The spectral resolving power was measured to be 1200, for a velocity resolution of 250km/s, as predicted from the known performance of the Fabry-Perot. The Fabry-Perot spectrum follows an Airy function to within a few percent, with no detectable excess crosstalk. As seen in the illumination pattern in Fig. 8, there is some optical crosstalk induced by the grating.

The opacities at the zenith during the observing run were measured by skydips using both FIBRE and the CSO facility  $350 \mu\text{m}$  taumeter. These measurements yielded zenith opacities of  $\tau_{350 \mu\text{m}} \sim 4$  during most of the run. A representative skydip under the best conditions seen is shown in Fig. 11. In this case, we found  $\tau_{372 \mu\text{m}} \sim 3.0 \pm 0.3$  measured using FIBRE operating at  $372 \mu\text{m}$ .

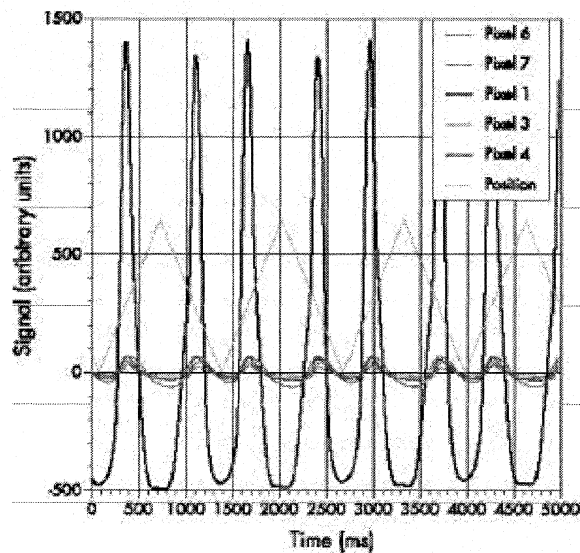


FIGURE 9. Multiplexed readout of the FIBRE bolometers.

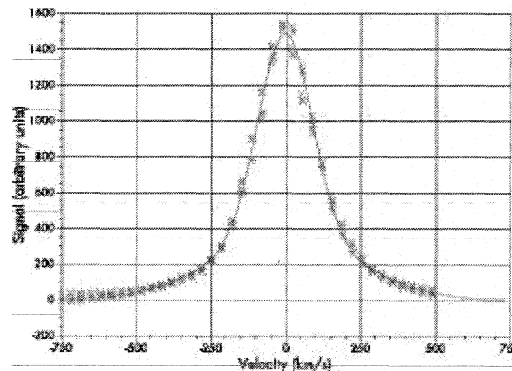


FIGURE 10. Velocity calibration spectrum at  $372 \mu\text{m}$  (807 GHz).

No scientific data could be taken in such poor conditions, but in order to demonstrate a multiplexed detection using TES bolometers, we observed the limb of the Moon at  $365\mu\text{m}$ . The secondary mirror was nutated to subtract the atmosphere, so we obtained a high signal-to-noise detection of the Moon emission despite a transmission of  $\sim 1\%$  (Fig. 12). The signal was demodulated and a signal-to-noise measured for each of the 11 scan positions. Each data point contains 3 seconds of on-source time. When pointing at the limb of the Moon, the chopping demodulation results in a difference signal between the Moon and the background sky.

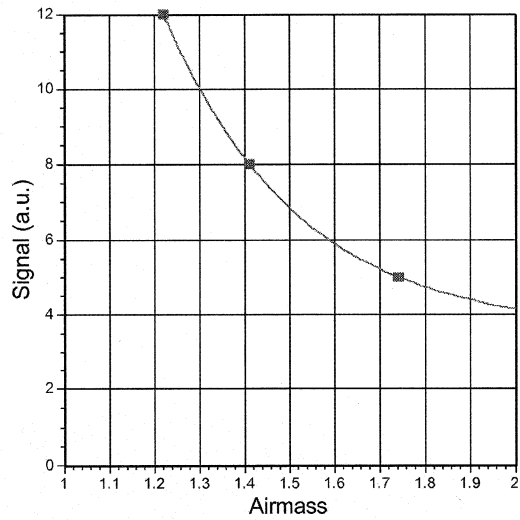


FIGURE 11. Skydip showing  $\tau_{372\mu\text{m}} \sim 3$ .

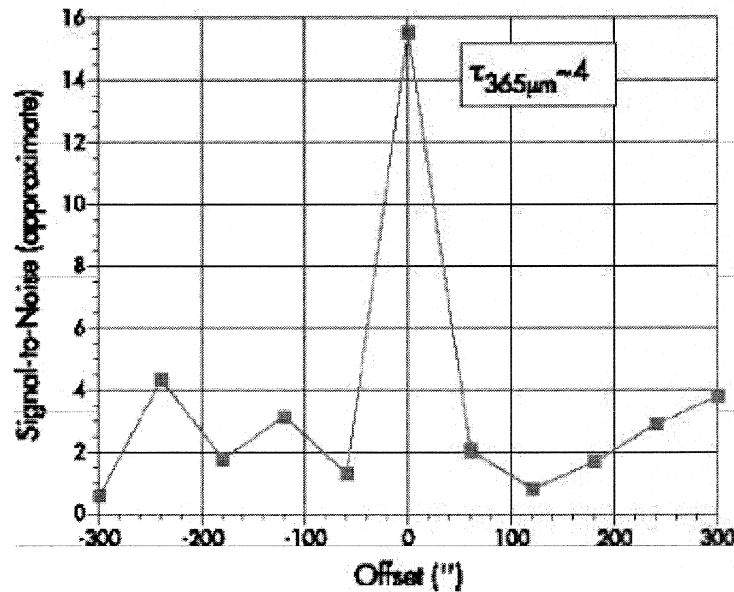


FIGURE 12. Detection of the limb of the Moon, taken while chopping so that a signal is seen only when exactly on the limb.

With the initial observations and instrument checkout, it is possible to predict the sensitivity of FIBRE to extragalactic line emission. First, a model of the atmosphere is used to estimate the noise equivalent flux (NEF) as a function of the 225 GHz opacity (Fig.

13). Second, assumptions about the total flux in a line from a galaxy is estimated, resulting in a minimum observation time calculation (Fig. 14).

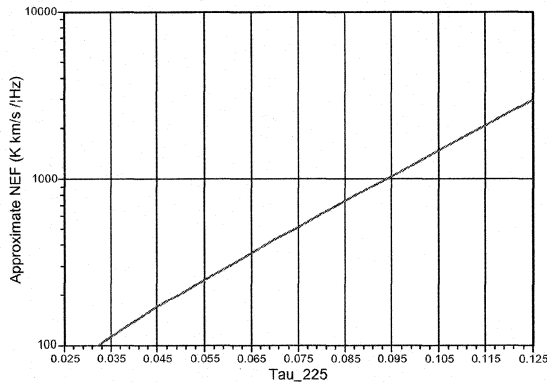


FIGURE 13. Prediction of the noise equivalent flux as a function of 225 GHz opacity.

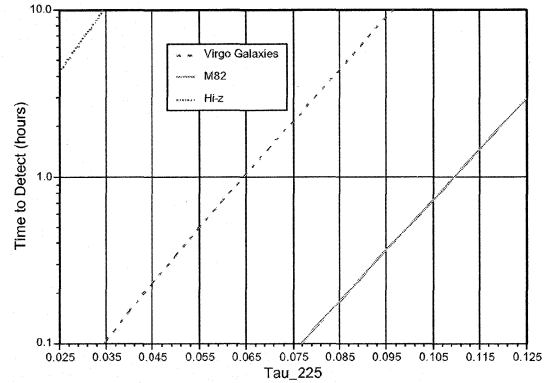


FIGURE 14. Time required to detect galaxy emission lines, as a function of 225 GHz opacity.

## CONCLUSION

FIBRE achieved first light at the CSO, detecting the Moon at  $365\mu\text{m}$  in bad weather with an atmospheric transmission of  $\sim 1\%$ . The spectrometer was operating with a spectral resolving power of  $\sim 1200$ , and the signal amplitude and noise were consistent with expectations. The TES bolometer and SQUID multiplexer technology has been thus validated in an astronomical application. The use of a direct detector in a high resolution spectrometer permits the testing of detectors with lower noise than is required for ground-based continuum instruments, thereby validating technology more suitable for space-based instruments. This work is a first step in the direction of placing superconducting bolometer arrays on a cryogenic space telescope, with the promise of orders of magnitude improvement in science output over previous missions. Because this is only a first step, much work remains to be done on all aspect of the system. We anticipate future observations to study galaxies in the fine-structure line of CI and the CO rotational lines, and to continue to refine the multiplexed TES detectors in astronomical applications.

## ACKNOWLEDGMENTS

We thank the staff of the CSO and our co-observers for making the observations described here possible; their support was crucial in the commissioning of FIBRE. We owe a debt of gratitude to many at NASA/GSFC, Caltech, IAS, and NIST for their contributions to FIBRE hardware and software.

## REFERENCES

1. Benford, D.J., Cox, P., Omont, A., Phillips, T.G. & McMahon, R.G., ApJ L518, 65 (1999).
2. Blain, A.W., Frayer, D.T., Bock, J.J., & Scoville, N.Z., MNRAS 313 (3), 559-570 (2000).
3. Schilke, P., Benford, D. J., Hunter, T. R., Lis, D. C., & Phillips, T. G., ApJS 132, 281 (2001)
4. Zmuidzinas, J., in "New Concepts for Far-Infrared and Submillimeter Space Astronomy", Leisawitz & Benford, eds., in press
5. Benford, D.J. et al., ASP Conference Series 217, 134-139 (1999).
6. Chervenak, J.A, et al, Appl. Phys. Letters 74 (26), 4043 (1999).
7. Benford, D.J., et al., Proceedings of 12<sup>th</sup> International Symposium on Space Terahertz Technology, JPL Publication 01-18, p.122
8. Benford, D.J., et al., Int. J. IR MM Waves 21 (12), 1909-1916 (2000).
9. Staguhn, J.G., et al., in "Low Temperature Detectors", F.S. Porter et al., eds., AIP Conference Proceedings #605, p.321.
10. Phillips, T.G. 1988, in "Millimetre and Submillimeter Astronomy", Wolstencroft & Burton, eds., p.1
11. Maffei, B., et al., Infrared Physics & Technology 35, 321 (1994).

